pp. 1843-1866

# SPATIAL PATTERN FORMATION IN ACTIVATOR-INHIBITOR MODELS WITH NONLOCAL DISPERSAL

### SHANSHAN CHEN\*

Department of Mathematics, Harbin Institute of Technology Weihai, Shandong 264209, China

#### Junping Shi

Department of Mathematics, William & Mary Williamsburg, Virginia, 23187-8795, USA

## GUOHONG ZHANG

School of Mathematics and Statistics, Southwest University Chongqing 400715, China

(Communicated by Feng-Bin Wang)

Dedicated to Professor Sze-Bi Hsu

ABSTRACT. The stability of a constant steady state in a general reaction-diffusion activator-inhibitor model with nonlocal dispersal of the activator or inhibitor is considered. It is shown that Turing type instability and associated spatial patterns can be induced by fast nonlocal inhibitor dispersal and slow activator diffusion, and slow nonlocal activator dispersal also causes instability but may not produce stable spatial patterns. The existence of nonconstant positive steady states is shown through bifurcation theory. This suggests a new mechanism for spatial pattern formation, which has different instability parameter regime compared to Turing mechanism. The theoretical results are applied to pattern formation problems in nonlocal Klausmeier-Gray-Scott water-plant model and Holling-Tanner predator-prey model.

1. **Introduction.** Reaction-diffusion models have been proposed to describe the emergence of self-organized pattern formations observed in the natural world or scientific experiments. Turing's pioneer work [50] suggested that different diffusion rates of activator and inhibitor in a biological system can lead to the generation of spatially inhomogeneous patterns, and such diffusion-induced instability (Turing instability) has been credited as the driving mechanism of pattern formations in chemistry [25, 37], developmental biology [14, 22, 45, 46], and ecology [19, 40, 41]. Mathematical theory of linear stability and symmetry-breaking bifurcation have

 $<sup>2020\</sup> Mathematics\ Subject\ Classification.$  Primary: 35K57, 35B32; Secondary: 35B35, 35B36, 37L15, 92C15.

 $Key\ words\ and\ phrases.$  Nonlocal dispersal, activator-inhibitor system, spatial pattern formation, bifurcation.

S. Chen is supported by National Natural Science Foundation of China (No 11771109), and J. Shi is supported by US-NSF grants DMS-1715651 and DMS-1853598, G. Zhang is supported by National Natural Science Foundation of China (No 11701472).

<sup>\*</sup> Corresponding author: Shanshan Chen.

been applied to the such reaction-diffusion models to rigorously establish the existence and stability of spatial patterns, see [16, 17, 27, 35, 38, 52, 53, 54] and references therein. In the framework of reaction-diffusion model, it is well-established that the condition for spatial pattern formation in two-species model is to have a slow diffusion rate for activator and a fast diffusion rate for inhibitor [14, 23].

While the diffusion equation with Laplace operator is the most commonly used mathematical model for substance passive movement in space, other spatial movement models have been identified and proposed in recent years. Usually such models are of nonlocal nature contrasting to the local one for the linear diffusion equation. In nonlocal dispersal models, the movement of individuals of biological species is often described by a linear integral operator in a continuous spatial landscape, and the underlying physical mechanism and mathematical theory are quite different from the ones for linear diffusion equation.

A commonly used integral operator for nonlocal dispersal is

$$\mathcal{P}u := c \left[ \frac{1}{l} \int_{-\infty}^{\infty} k \left( \frac{x - y}{l} \right) u(y) dy - u(x) \right], \tag{1}$$

where l is a spatial scale representing the dispersal distance; k is a non-negative symmetric function satisfying  $\int_{-\infty}^{\infty} k(x)dx = 1$ , and k(x-y) is the probability to jump from one location x to another y. This nonlocal diffusion operator (1) could be used to model plant seed dispersal [39], weed dispersal [2, 3], disease spread [34] or population movements [30], see [1, 5, 12, 15, 24] for studies of spatial population models with nonlocal dispersal.

As pointed out in [26], the nonlocal dispersal operator  $\mathcal{L}$  could be approximated by the standard diffusion operator (respectively, the "spatial averaging" dispersal operator) for small l (respectively, large l). For the case that l is small,

$$\begin{split} \mathcal{P}u = & c \left[ \frac{1}{l} \int_{-\infty}^{\infty} k \left( \frac{x-y}{l} \right) u(y) dy - u(x) \right] = c \left[ \frac{1}{l} \int_{-\infty}^{\infty} k(z) u(x-zl) dz - u(x) \right] \\ = & \frac{cl^2}{2} \left( \int_{-\infty}^{\infty} k(z) z^2 dz \right) \frac{\partial^2 u}{\partial x^2} + O(l^3). \end{split}$$

Then the nonlocal dispersal operator  $\mathcal{L}$  could be approximated by a diffusion operator for the small spreading scale l. One the other hand, for the case that l is large, if the density u(x) is periodic in x with period L, then

$$\mathcal{P}u = c \int_0^L \left[ \frac{1}{l} \sum_{i=-\infty}^{\infty} k \left( \frac{x+iL}{l} \right) \right] u(y) dy.$$

Then, formally,

$$\frac{1}{l} \sum_{i=-\infty}^{\infty} k\left(\frac{x+iL}{l}\right) \to \frac{1}{L} \int_{-\infty}^{\infty} k(y) dy = \frac{1}{L},$$

as  $l \to \infty$ . Therefore, for the large spreading scale l, the nonlocal dispersal could be approximated by the following "spatial averaging" dispersal operator

$$\mathcal{P}_1 u = c \left( \frac{1}{L} \int_0^L u(y) dy - u(x) \right). \tag{2}$$

This simplified nonlocal dispersal operator  $\mathcal{P}_1$  means biologically that the movement distance of the species is much larger than the diameter of the habitat or the size of home range, see [26].

A natural question is how the nonlocal dispersal affects the spatial pattern formation and whether the nonlocal dispersal could also induce complex patterns as the Turing instability theory for the diffusion type dispersal. In this paper, we give an affirmative answer to this question for the simplified nonlocal dispersal operator  $\mathcal{P}_1$ . For simplicity we assume the spatial domain to be one-dimensional. We propose the following reaction-diffusion model with one species disperses nonlocally and general kinetic.

$$\begin{cases} \frac{\partial u}{\partial t} = c \left( \frac{1}{L} \int_0^L u(y, t) dy - u(x, t) \right) + f(u, v), & 0 \le x \le L, \ t > 0, \\ \frac{\partial v}{\partial t} = dv_{xx} + g(u, v), & 0 < x < L, \ t > 0, \\ v_x(0, t) = v_x(L, t) = 0, & t > 0, \end{cases}$$

$$(3)$$

where u(x,t) and v(x,t) are the density functions of two biological or chemical species at time t and location x, and the spatial domain is an interval [0,L] for some L>0; the first species u disperses following the nonlocal averaging strategy  $\frac{1}{L}\int_0^L u(y,t)dy-u(x,t)$  with a dispersal coefficient c>0, and the second species v follows the passive diffusion strategy  $v_{xx}(x,t)$  with diffusion coefficient d>0; and the functions f(u,v),g(u,v) are smooth ones defined for  $u,v\geq 0$  which describe chemical reactions or biological growth and interactions. The nonlocal dispersal in (3) was used in [4, 26] for a Lotka-Volterra competition model with nonlocal dispersal, and a reaction-diffusion water-plant interaction model with plant nonlocal dispersal in form of (3) was considered in [12]. The system (3) is in a more general form allowing all possible reaction or interaction dynamics. We also assume that the model (3) has a constant positive steady state  $(u_*, v_*)$  satisfying  $f(u_*, v_*) = g(u_*, v_*) = 0$ , which is linearly stable for the corresponding ODEs. The question is whether a combination of the nonlocal dispersal of u and local dispersal of v can produce non-trivial spatial patterns.

The model (3) is compared to the corresponding classical reaction-diffusion activator inhibitor system:

$$\begin{cases} \frac{\partial u}{\partial t} = cu_{xx} + f(u, v), & 0 < x < L, \ t > 0, \\ \frac{\partial v}{\partial t} = dv_{xx} + g(u, v), & 0 < x < L, \ t > 0, \\ u_x(0, t) = u_x(L, t) = 0, \ v_x(0, t) = v_x(L, t) = 0, \ t > 0. \end{cases}$$
(4)

If  $(u_*, v_*)$  is linearly stable with respect to the corresponding ODE kinetic system, then

$$f_u(u_*, v_*) + g_v(u_*, v_*) < 0, \quad f_u(u_*, v_*)g_v(u_*, v_*) - f_v(u_*, v_*)g_u(u_*, v_*) > 0.$$
 (5)

For simplicity of notations, throughout this paper, we use  $f_u$ ,  $f_v$ ,  $g_u$  and  $g_v$  to represent the first order partial derivatives of f and g at  $(u_*, v_*)$  respectively. If the Turing instability occurs for (4), the Jacobian matrix

$$J = \begin{pmatrix} f_u & f_v \\ g_u & g_v \end{pmatrix} \tag{6}$$

at  $(u_*, v_*)$  must have the one of the following sign patterns:

$$(a)\begin{pmatrix} + & + \\ - & - \end{pmatrix}, (b)\begin{pmatrix} + & - \\ + & - \end{pmatrix}, (c)\begin{pmatrix} - & + \\ - & + \end{pmatrix}, (d)\begin{pmatrix} - & - \\ + & + \end{pmatrix}.$$
 (7)

Here  $f_u$  and  $g_v$  have opposite signs, and we call u (respectively, v) an activator if  $f_u$  (respectively,  $g_v$ ) is positive, whereas u (respectively, v) is a inhibitor if  $f_u$  (respectively,  $g_v$ ) is negative. That is, the activator activates its own production while inhibitor inhibits its own production. For (4), pattern (b) and (c) are equivalent if one switches the labelling of u and v, and it is called activator-inhibitor type; and (a) and (d) are equivalent if one switches the labelling of u and v, and it is called activator-depletion (or substrate depletion) type [14, 42].

For both the activator-inhibitor type and activator-depletion type, the constant steady state loses the stability when the diffusion of activator is slow and the one for inhibitor is fast, and spatially non-constant steady states (patterns) of the reaction-diffusion system (4) bifurcate from the constant one, see [6, 16, 17, 27, 28, 35, 38] and references therein. Our main results for spatial pattern formation in the model with nonlocal dispersal (3) can be summarized as follows:

- When the dispersal of the activator is nonlocal and the one for the inhibitor is diffusive (schemes (a) or (b) in (7)), the constant steady state  $(u_*, v_*)$  is always linearly stable with respect to (3) if the activator dispersal is fast, and it is always linearly unstable if the activator dispersal is slow. Here the diffusion rate of the inhibitor does not affect the stability. But the instability caused by slow activator dispersal in this case may not lead to spatial pattern formation as the unstable space of the constant steady state is always infinite dimensional, and any non-constant steady states generated from symmetry-breaking bifurcations are unstable as well. This is similar to the pattern formation scenario of coupled ODE-PDE systems, which corresponds to the case of immobile activator with no dispersal, see [29, 32].
- When the dispersal of the activator is diffusive and the one for the inhibitor is nonlocal (schemes (c) or (d) in (7)), the constant steady state  $(u_*, v_*)$  is always linearly stable with respect to (3) if the inhibitor dispersal is slow or the inhibitor dispersal is fast and the activator diffusion is also fast, and it is linearly unstable if the inhibitor dispersal is fast and the activator diffusion is slow. The latter case is similar to the Turing instability for the classical reaction-diffusion model (4). The unstable space of the constant steady state is finite dimensional, and the non-constant steady states generated from symmetry-breaking bifurcations could be stable ones. Hence the fast nonlocal dispersal of the inhibitor and slow activator diffusion can induce spatial pattern formation, which is a pattern-forming mechanism different from the Turing mechanism.

We point out that the nonlocal dispersal with other assumptions on the kernel has also been investigated, see [8, 9, 13, 44, 47, 48] and references therein.

The rest of the paper is organized as follows. In Section 2, we obtain the existence of nonconstant positive steady states of model (3) through bifurcation theory, and show the effect of dispersal rate on the diffusion-induced bifurcations. In Section 3, we apply the obtained theoretical results in Section 2 to the nonlocal Klausmeier-Gray-Scott model and Holling-Tanner predator-prey model, and some numerical simulations are given to show the complex pattern formation. Throughout the paper, we denote the set of complex numbers by  $\mathbb{C} = \{x + iy : x, y \in \mathbb{R}\}$ ,  $\mathbb{C}^- = \{x + iy : x, y \in \mathbb{R}\}$ ,  $\mathbb{C}^- = \{x + iy : x, y \in \mathbb{R}\}$ ,  $\mathbb{C}^- = \{x + iy : x, y \in \mathbb{R}\}$ ,  $\mathbb{C}^- = \{x + iy : x, y \in \mathbb{R}\}$ ,  $\mathbb{C}^- = \{x + iy : x, y \in \mathbb{R}\}$ 

 $\{x+iy: x,y \in \mathbb{R}, x < 0\}$ , and  $\mathbb{C}^+ = \{x+iy: x,y \in \mathbb{R}, x > 0\}$ . For a linear operator L, we denote the domain of L by  $\mathscr{D}(L)$ , the range of L by  $\mathscr{R}(L)$ , the kernel of L by  $\mathscr{N}(L)$ , the resolvent set of L by  $\rho(L)$ , and the spectrum, point spectrum and continuous spectrum of L by  $\sigma(L)$ ,  $\sigma_p(L)$  and  $\sigma_c(L)$ , respectively.

2. Steady states and bifurcation analysis. In this section, we aim to consider the existence of nonconstant positive steady states of model (3), which satisfy

$$\begin{cases} c\left(\frac{1}{L}\int_{0}^{L}u(y)dy - u(x)\right) + f(u(x), v(x)) = 0, & 0 \le x \le L, \\ dv''(x) + g(u(x), v(x)) = 0, & 0 < x < L, \\ v'(0) = v'(L) = 0. \end{cases}$$
(8)

We assume that system (3) has a positive constant steady state  $(u_*, v_*)$  which is linearly stable with respect to the corresponding ODE system, that is, the Jacobian matrix J in (6) satisfies (5). Moreover if the Turing instability could occur with respect to the reaction-diffusion system (4), the sign pattern of the Jacobian matrix (6) at  $(u_*, v_*)$  must belong to one of the four schemes (a), (b), (c) or (d) defined in Eq. (7).

Let 
$$X = C([0, L]) \times C_N^2([0, L])$$
 and  $Y = C([0, L]) \times C([0, L])$ , where  $C_N^2([0, L]) = \{u \in C^2([0, L]) : u'(0) = u'(L) = 0\}.$ 

Denote the linearized operator of (8) at  $(u_*, v_*)$  by

$$\mathcal{L}\begin{pmatrix} \phi \\ \psi \end{pmatrix} = \begin{pmatrix} c\mathcal{K}\phi + f_u\phi + f_v\psi \\ d\psi'' + g_u\phi + g_v\psi \end{pmatrix},\tag{9}$$

where

$$\mathcal{K}\phi = \frac{1}{L} \int_0^L \phi dx - \phi. \tag{10}$$

Clearly,  $\mathcal{L}$  is a closed linear operator in Y with domain  $D(\mathcal{L}) = X$ . We first consider the spectrum of operator  $\mathcal{K}$  for further application.

**Lemma 2.1.** Let  $K : C([0,L]) \to C([0,L])$  be defined in Eq. (10). Then  $\sigma(K) = \sigma_p(K) = \{0,-1\}.$ 

*Proof.* Define  $\mathcal{K}_1: C([0,L]) \to C([0,L])$  by

$$\mathcal{K}_1 \phi = \frac{1}{L} \int_0^L \phi dx. \tag{11}$$

Then  $\mathcal{K}_1$  is a compact operator on C([0,L]), which implies that

$$0 \in \sigma(\mathcal{K}_1)$$
, and  $\sigma(\mathcal{K}_1) \setminus \{0\} = \sigma_p(\mathcal{K}_1) \setminus \{0\}$ .

Clearly,

$$\mathcal{N}(\mathcal{K}_1) = \left\{ \phi \in C([0, L]) : \frac{1}{L} \int_0^L \phi dx = 0 \right\} \neq \emptyset,$$

which yields  $0 \in \sigma_p(\mathcal{K}_1)$ . Let  $\lambda \in \sigma_p(\mathcal{K}_1) \setminus \{0\}$ , and let  $\phi \in C([0, L])$  be the corresponding eigenfunction associated with  $\lambda$ . Then

$$\frac{1}{\lambda L} \int_0^L \phi dx = \phi,$$

and consequently, there exists a nonzero constant  $c \in \mathbb{C}$  such that  $\phi \equiv c$ . Therefore,  $\lambda = 1$ , and  $\sigma(\mathcal{K}_1) = \sigma_p(\mathcal{K}_1) = \{0, 1\}$ . It follows that  $\sigma(\mathcal{K}) = \sigma_p(\mathcal{K}) = \{0, -1\}$ . This completes the proof.

Next we consider the spectrum of the linearized operator  $\mathcal{L}$  by using Lemma 2.1 and methods motivated by the ones in [29].

**Theorem 2.2.** Assume that  $(u_*, v_*)$  is a constant positive steady state of model (3). Suppose that c, d > 0,  $f_v g_u \neq 0$ , and let  $\ell_n = \frac{n^2 \pi^2}{L^2}$  for  $n = 1, 2, 3, \cdots$ . Then  $\sigma(\mathcal{L}) = S_1 \cup S_2$ , where  $S_1$  and  $S_2$  satisfy the following.

(i) 
$$S_1 = \sigma_p(\mathcal{L}) = \{\lambda_n\}_{n=0}^{\infty} \cup \{\mu_n\}_{n=0}^{\infty}, \text{ where }$$

$$\lambda_{0} = \frac{1}{2} \left( f_{u} + g_{v} - \sqrt{(f_{u} - g_{v})^{2} + 4f_{v}g_{u}} \right),$$

$$\mu_{0} = \frac{1}{2} \left( f_{u} + g_{v} + \sqrt{(f_{u} - g_{v})^{2} + 4f_{v}g_{u}} \right),$$

$$\lambda_{n} = \frac{1}{2} \left( f_{u} + g_{v} - c - d\ell_{n} - \sqrt{(f_{u} + d\ell_{n} - c - g_{v})^{2} + 4f_{v}g_{u}} \right),$$

$$\mu_{n} = \frac{1}{2} \left( f_{u} + g_{v} - c - d\ell_{n} + \sqrt{(f_{u} + d\ell_{n} - c - g_{v})^{2} + 4f_{v}g_{u}} \right),$$
(12)

for  $n = 1, 2, 3, \cdots$ . Furthermore,

$$(\phi_{0,-},\psi_{0,-}) = \left(\frac{f_v}{\lambda_0 - f_u}, 1\right), \quad (\phi_{0,+},\psi_{0,+}) = \left(\frac{f_v}{\mu_0 - f_u}, 1\right) \tag{13}$$

are eigenfunctions corresponding to  $\lambda_0$  and  $\mu_0$  respectively, and for  $n \geq 1$ ,

$$(\phi_{n,-}, \psi_{n,-}) = \left(\frac{f_v}{\lambda_n + c - f_u} \cos \frac{n\pi x}{L}, \cos \frac{n\pi x}{L}\right),$$

$$(\phi_{n,+}, \psi_{n,+}) = \left(\frac{f_v}{\mu_n + c - f_u} \cos \frac{n\pi x}{L}, \cos \frac{n\pi x}{L}\right)$$
(14)

are eigenfunctions corresponding to  $\lambda_n$  and  $\mu_n$  respectively.

(ii) 
$$S_2 = \{f_u - c\}$$
. Furthermore,  $S_2 = \sigma_c(\mathcal{L})$  if  $c(g_v - f_u + c) - f_v g_u \neq 0$ , and if  $c(g_v - f_u + c) - f_v g_u = 0$ , then  $f_u - c = \lambda_0$  or  $\mu_0$ , and  $f_u - c \in \sigma_p(\mathcal{L})$ .

Proof. Consider the linear resolvent equation,

$$\mathcal{L}\begin{pmatrix} \phi \\ \psi \end{pmatrix} = \lambda \begin{pmatrix} \phi \\ \psi \end{pmatrix} + \begin{pmatrix} \tau_1 \\ \tau_2 \end{pmatrix}, \text{ where } (\tau_1, \tau_2) \in Y, \tag{15}$$

which is equivalent to

$$\begin{cases}
c\mathcal{K}\phi + f_u\phi + f_v\psi = \lambda\phi + \tau_1, \\
d\psi'' + g_u\phi + g_v\psi = \lambda\psi + \tau_2, \\
\psi'(0) = \psi'(L) = 0.
\end{cases}$$
(16)

It follows from Lemma 2.1 that if  $\lambda \notin \{f_u, f_u - c\}$ , then  $c\mathcal{K} + (f_u - \lambda)I$  has a bounded inverse, where  $I: C([0, L]) \to C([0, L])$  is the identity operator, and if  $\lambda = f_u$  or  $f_u - c$ , then  $c\mathcal{K} + (f_u - \lambda)I$  does not have a bounded inverse. Therefore, we will divide our discussion into three cases.

Case 1. We first consider the case of  $\lambda = f_u$ . Substituting  $\lambda = f_u$  into (16), we have

$$\begin{cases}
c\left(\frac{1}{L}\int_{0}^{L}\phi dy - \phi\right) + f_{v}\psi = \tau_{1}, \\
d\psi'' + g_{u}\phi + (g_{v} - f_{u})\psi = \tau_{2}, \\
\psi'(0) = \psi'(L) = 0.
\end{cases}$$
(17)

Integrating the first two equations of (17) over [0, L], we have

$$\int_{0}^{L} \psi dx = \frac{\int_{0}^{L} \tau_{1} dx}{f_{v}} \text{ and } g_{u} \int_{0}^{L} \phi dx + (g_{v} - f_{u}) \int_{0}^{L} \psi dx = \int_{0}^{L} \tau_{2} dx,$$

which yield

$$\int_{0}^{L} \phi dx = \frac{1}{g_u} \left( \int_{0}^{L} \tau_2 dx - \frac{g_v - f_u}{f_v} \int_{0}^{L} \tau_1 dx \right). \tag{18}$$

This, combined with the first equation of (17), implies that

$$\phi = -\frac{\tau_1}{c} + \frac{f_v}{c}\psi + \frac{1}{g_u L} \left( \int_0^L \tau_2 dx - \frac{g_v - f_u}{f_v} \int_0^L \tau_1 dx \right). \tag{19}$$

Substituting (19) into the second equation of (17), we get

$$\mathcal{J}_1 \psi := d\psi'' + \frac{f_v g_u}{c} \psi + (g_v - f_u) \psi = \tau_2 + \frac{g_u \tau_1}{c} - \frac{1}{L} \left( \int_0^L \tau_2 dx - \frac{g_v - f_u}{f_v} \int_0^L \tau_1 dx \right). \tag{20}$$

The following discussion for this case is divided into three subcases.

**Subcase 1a.** If  $c(g_v - f_u - d\ell_n) + f_v g_u \neq 0$  for any  $n = 0, 1, 2, \dots$ , the operator  $\mathcal{J}_1$  has a bounded inverse on C([0, L]), which implies that  $\mathcal{L} - f_u I$  has a bounded inverse  $(\mathcal{L} - f_u I)^{-1}$  on Y, and it follows that  $f_u \in \rho(\mathcal{L})$ .

**Subcase 1b.** If  $c(g_v - f_u) + f_v g_u = 0$ , then the integral of the right hand side of Eq. (20) over [0, L] is zero. Note that the operator  $\mathcal{J}_1$  has a bounded inverse on  $\{\phi \in C([0, L] : \int_0^L \phi dx = 0\}$ . Then, in this case, we also obtain that  $\mathcal{L} - f_u I$  has a bounded inverse  $(\mathcal{L} - f_u I)^{-1}$  on Y, and  $f_u \in \rho(\mathcal{L})$ .

**Subcase 1c.** If  $c(g_v - f_u - d\ell_n) + f_v g_u = 0$  for some positive integer n, letting  $\tau_1 \equiv \tau_2 \equiv 0$  in (17), we see that the kernel of  $\mathcal{L} - f_u I$  is

$$\mathcal{N}(\mathcal{L} - f_u I) = span\left\{ \left( \frac{f_v}{c} \cos \frac{n\pi x}{L}, \cos \frac{n\pi x}{L} \right) \right\},$$

and consequently,  $f_u \in \sigma_p(\mathcal{L})$  and  $\left(\frac{f_v}{c}\cos\frac{n\pi x}{L},\cos\frac{n\pi x}{L}\right)$  is the corresponding eigenfunction with respect to  $\lambda = f_u$ .

Case 2. Next we consider the case that  $\lambda = f_u - c$ . Substituting  $\lambda = f_u - c$  into (16), we have

$$\begin{cases} \frac{c}{L} \int_{0}^{L} \phi dx + f_{v}\psi = \tau_{1}, \\ d\psi'' + g_{u}\phi + (g_{v} - f_{u} + c)\psi = \tau_{2}, \\ \psi'(0) = \psi'(L) = 0. \end{cases}$$
(21)

Integrating the first two equations of (21) over [0, L], we have

$$c \int_{0}^{L} \phi dx + f_{v} \int_{0}^{L} \psi dx = \int_{0}^{L} \tau_{1} dx,$$

$$g_{u} \int_{0}^{L} \phi dx + (g_{v} - f_{u} + c) \int_{0}^{L} \psi dx = \int_{0}^{L} \tau_{2} dx.$$
(22)

The following discussion for this case is also divided into two subcases. **Subcase 2a.** If  $c(g_v - f_u + c) - f_v g_u \neq 0$ , then

$$\int_{0}^{L} \phi dx = \frac{f_{v} \int_{0}^{L} \tau_{2} dx - (g_{v} - f_{u} + c) \int_{0}^{L} \tau_{1} dx}{f_{v} g_{u} - c(g_{v} - f_{u} + c)},$$

$$\int_{0}^{L} \psi dx = \frac{g_{u} \int_{0}^{L} \tau_{1} dx - c \int_{0}^{L} \tau_{2} dx}{f_{v} g_{u} - c(g_{v} - f_{u} + c)}.$$
(23)

Substituting Eq. (23) into (21), we have

$$\psi = \frac{\tau_1}{f_v} - \frac{c}{f_v L} \frac{f_v \int_0^L \tau_2 dx - (g_v - f_u + c) \int_0^L \tau_1 dx}{f_v g_u - c(g_v - f_u + c)},$$

$$\phi = \frac{1}{g_u} \left[ \tau_2 - (g_v - f_u + c)\psi - d\psi'' \right].$$
(24)

It follows that  $\mathcal{L} - (f_u - c)I$  is injective and the range  $\mathcal{R}(\mathcal{L} - (f_u - c)I) = C_N^2([0, L]) \times C([0, L])$ , which is dense in Y. Therefore  $\lambda = f_u - c$  is in the continuous spectrum  $\sigma_c(\mathcal{L})$ .

**Subcase 2b.** Now we consider the case that  $c(g_v - f_u + c) - f_v g_u = 0$ . Let  $\tau_1 \equiv \tau_2 \equiv 0$  in (21), and then we see that  $\phi$  and  $\psi$  are constant functions, which implies that the kernel of  $\mathcal{L} - (f_u - c)I$  is

$$\mathcal{N}(\mathcal{L} - (f_u - c)I) = span\left\{\left(-\frac{f_v}{c}, 1\right)\right\},\,$$

and  $\lambda = f_u - c \in \sigma_p(\mathcal{L})$ .

Case 3. Finally, we consider the case that  $\lambda \notin \{f_u, f_u - c\}$ . Then

$$\phi = [c\mathcal{K} + (f_u - \lambda)I]^{-1}[\tau_1 - f_v\psi]. \tag{25}$$

Substituting Eq. (25) into the second equation of (16), we get

$$d\psi'' + g_u[c\mathcal{K} + (f_u - \lambda)I]^{-1}[\tau_1 - f_v\psi] + g_v\psi = \lambda\psi + \tau_2,$$

which is equivalent to

$$\mathcal{J}_2\psi = \tilde{\tau},\tag{26}$$

where

$$\mathcal{J}_{2}\psi := d\psi'' + \frac{c(g_{v} - \lambda)}{L(f_{u} - \lambda - c)} \int_{0}^{L} \psi dx + \frac{(g_{v} - \lambda)(f_{u} - c - \lambda) - g_{u}f_{v}}{f_{u} - \lambda - c} \psi,$$

$$\tilde{\tau} := \frac{1}{f_{u} - \lambda - c} [c\mathcal{K} + (f_{u} - \lambda)I]\tau_{2} - \frac{g_{u}}{f_{u} - \lambda - c}\tau_{1}.$$
(27)

Note that  $\mathcal{K}_1\psi = \frac{1}{L} \int_0^L \psi dx$  is a bounded linear operator in C([0, L]). It follows from [36, Chapter 3, Proposition 1.4 and Corollary 2.2] that  $\mathcal{J}_2$  is the infinitesimal generator of an analytic and compact semigroup on C([0, L]) with domain  $\mathcal{D}(\mathcal{J}_2) = \mathcal{D}([0, L])$ 

 $C_N^2([0,L])$ . Then, we obtain that  $\sigma(\mathcal{J}_2) = \sigma_p(\mathcal{J}_2)$  from [36, Chapter 2, Corollary 3.7]. A direct calculation implies that

$$\sigma_p(\mathcal{J}_2) = \{s_0\} \cup \{s_n\}_{n=1}^{\infty},$$

where

$$s_{0} = \frac{1}{f_{u} - \lambda - c} \begin{vmatrix} \lambda - f_{u} & -f_{v} \\ -g_{u} & \lambda - g_{v} \end{vmatrix}$$

$$= \frac{1}{f_{u} - \lambda - c} \left[ \lambda^{2} - (f_{u} + g_{v})\lambda + f_{u}g_{v} - f_{v}g_{u} \right],$$

$$s_{n} = \frac{1}{f_{u} - \lambda - c} \begin{vmatrix} \lambda + c - f_{u} & -f_{v} \\ -g_{u} & \lambda + d\ell_{n} - g_{v} \end{vmatrix}$$

$$= \frac{1}{f_{u} - \lambda - c} \left[ \lambda^{2} - (f_{u} + g_{v} - c - d\ell_{n})\lambda + (c - f_{u})(d\ell_{n} - g_{v}) - f_{v}g_{u} \right],$$
(28)

for  $n = 1, 2, 3, \cdots$ . Then the following discussion for this case is divided into two subcases.

Subcase 3a. If  $0 \notin \sigma(\mathcal{J}_2)$ , that is

$$\lambda^{2} - (f_{u} + g_{v})\lambda + f_{u}g_{v} - f_{v}g_{u} \neq 0 \text{ and}$$

$$\lambda^{2} - (f_{u} + g_{v} - c - d\ell_{n})\lambda + (c - f_{u})(d\ell_{n} - g_{v}) - f_{v}g_{u} \neq 0 \text{ for } n = 1, 2, 3, \dots,$$
(29)

then  $\mathcal{J}_2$  has a bounded inverse  $\mathcal{J}_2^{-1}$  on C([0,L]) and

$$\|\psi\|_{\infty} \le \frac{1}{|f_u - \lambda - c|} \|\mathcal{J}_2^{-1}\| \left[ (2c + |f_u - \lambda|) \|\tau_2\|_{\infty} + |g_u| \|\tau_1\|_{\infty} \right],$$

and consequently,

$$\|\phi\|_{\infty} \leq \|[c\mathcal{K} + (f_u - \lambda)I]^{-1}\| (\|\tau_1\|_{\infty} + |f_v|\|\psi\|_{\infty}).$$

Therefore,  $\mathcal{L} - \lambda I$  has a bounded inverse  $(\mathcal{L} - \lambda I)^{-1}$  on Y, and it follows that  $\lambda \in \rho(\mathcal{L})$ .

**Subcase 3b.** If  $0 \in \sigma(\mathcal{J}_2)$ , then  $\lambda$  satisfies the characteristic equation

$$\lambda^{2} - (f_{u} + g_{v})\lambda + f_{u}g_{v} - f_{v}g_{u} = 0, \tag{30}$$

or

$$\lambda^{2} - (f_{u} + g_{v} - c - d\ell_{n})\lambda + (c - f_{u})(d\ell_{n} - g_{v}) - f_{v}g_{u} = 0$$
(31)

for some integer  $n \geq 1$ . A direct computation implies that Eq. (30) has two roots  $\lambda_0$  and  $\mu_0$ , and Eq. (31) has two roots  $\lambda_n$  and  $\mu_n$  for  $n \geq 1$ , where  $\lambda_n, \mu_n$  ( $n = 0, 1, 2, \cdots$ ) are defined in Eq. (12). It follows from  $f_v g_u \neq 0$  that  $\lambda_0, \mu_0 \neq f_u$  and  $\lambda_n, \mu_n \neq f_u - c$  for any  $n \geq 1$ . Clearly,  $f_u$  satisfies Eq. (31) for some positive integer n if and only if  $c(g_v - f_u - d\ell_n) + f_v g_u = 0$  for some positive integer n. It follows from Subcase 1c that if  $c(g_v - f_u - d\ell_n) + f_v g_u = 0$  for some positive integer n, then  $f_u = \lambda_n$  or  $\mu_n$ , and  $\lambda_n, \mu_n \in \sigma_p(\mathcal{L})$ . Moreover,  $f_u - c$  satisfies Eq. (30) if and only if  $c(g_v - f_u + c) - f_v g_u = 0$ . It follows from Subcase 2b that if  $c(g_v - f_u + c) - f_v g_u = 0$ , then  $f_u - c = \lambda_0$  or  $\mu_0$ , and  $\lambda_0, \mu_0 \in \sigma_p(\mathcal{L})$ . Therefore,  $\lambda_n, \mu_n$  ( $n = 0, 1, 2, 3 \cdots$ ) are the eigenvalues of  $\mathcal{L}$ , ( $\phi_{0,-}, \psi_{0,-}$ ) and ( $\phi_{0,+}, \psi_{0,+}$ ) (defined in Eq. (13)) are the eigenfunctions corresponding to  $\lambda_0$  and  $\mu_0$  respectively, and for  $n \geq 1$ , ( $\phi_{n,-}, \psi_{n,-}$ ) and ( $\phi_{n,+}, \psi_{n,+}$ ) (defined in Eq. (14)) are the eigenfunctions corresponding to  $\lambda_n$  and  $\mu_n$  respectively.

It follows from the above three cases that  $\sigma(\mathcal{L}) = S_1 \cup S_2$ , and  $S_1$  and  $S_2$  satisfy (i) and (ii).

Theorem 2.2 shows that the spectrum of the linearized operator  $\mathcal{L}$  of (8) at a constant equilibrium can be completed determined. Note that the eigenvalues  $\lambda_n, \mu_n \ (n=0,1,2,3,\cdots)$  defined in Eq. (12) are not necessarily real numbers. The corresponding constant equilibrium  $(u_*, v_*)$  is linearly stable if all spectrum points have negative real parts, that is,  $\sigma(\mathcal{L}) \subset \mathbb{C}^-$ . Otherwise it is unstable. Then immediately from Theorem 2.2 (ii), we have

Corollary 1. Assume that  $(u_*, v_*)$  is a constant positive steady state of model (3). If  $c < f_u$ , then  $(u_*, v_*)$  is always unstable.

The instability stated in Corollary 1 holds for any constant steady state as long as the strength of the nonlocal dispersal is smaller than some threshold value. And it is also a generalization of Corollary 2.2 of [33], which is the case that c=0. Note that this result holds regardless of the stability of  $(u_*, v_*)$  with respect to the ODE dynamics, and it is also independent of d, the diffusion coefficient of the passive diffusive species.

Now we apply the general results in Theorem 2.2 to the activator-inhibitor system (3). First we consider the schemes (a) and (b) in (7), where the dispersal of the activator is nonlocal while the inhibitor has a diffusive dispersal. We have the following result on the stability of  $(u_*, v_*)$ .

**Theorem 2.3.** Assume that  $(u_*, v_*)$  is a constant positive equilibrium of model (3), the sign pattern of the Jacobian matrix (6) at  $(u_*, v_*)$  is either scheme (a) or (b) defined as in (7), and (5) is satisfied. Then the spectral set

$$\sigma(\mathcal{L}) = \{\lambda_n\}_{n=0}^{\infty} \cup \{\mu_n\}_{n=0}^{\infty} \cup \{f_u - c\},$$
 (32)

where  $\lambda_n, \mu_n$   $(n = 0, 1, 2, \cdots)$  are the eigenvalues defined in Eq. (12). Furthermore

- (i) If  $c > f_u$ , then  $\sigma(\mathcal{L}) \subset \mathbb{C}^-$  and  $(u_*, v_*)$  is linearly stable. (ii) If  $c = f_u$ , then  $\sigma(\mathcal{L}) = \sigma_p(\mathcal{L}) \cup \sigma_c(\mathcal{L})$ , where  $\sigma_p(\mathcal{L}) = \{\lambda_n\}_{n=0}^{\infty} \cup \{\mu_n\}_{n=1}^{\infty} \subset \{\mu_n\}_{n=1}^{\infty}$  $\mathbb{C}^-$ , and  $\sigma_c(\mathcal{L}) = \{0\}$ .
- (iii) If  $c < f_u$ , then  $\sigma(\mathcal{L}) = \sigma_p(\mathcal{L}) \cup \sigma_c(\mathcal{L})$ , where  $\sigma_c(\mathcal{L}) = \{f_u c\}, \ \sigma_p(\mathcal{L}) = \{f_u c\}, \ \sigma_p$  $\{\lambda_n\}_{n=0}^{\infty} \cup \{\mu_n\}_{n=1}^{\infty}$ , and  $\sigma_p(\mathcal{L}) \cap \mathbb{C}^+$  has infinitely many elements. Furthermore, there exists a positive sequence  $\{d_n\}_{n=1}^{\infty}$  defined by

$$d_n = \frac{f_u g_v - g_u f_v - c g_v}{(f_u - c)\ell_n} \quad for \quad n = 1, 2, 3, \cdots,$$
(33)

such that  $\mu_n > 0 > \lambda_n$  for any  $n \ge 1$  when  $d > d_1$ , and when  $d \in (d_{n+1}, d_n)$ ,  $\mu_j > 0 > \lambda_j$  for any  $j \ge n+1$  and  $0 > \mu_j > \lambda_j$  for any  $j \le n$ .

*Proof.* It follows from Eq. (5) that if  $c \leq f_u$ , then  $c(g_v - f_u + c) - f_v g_u > 0$ . This, combined with Theorem 2.2, implies that  $\sigma_c(\mathcal{L}) = \{f_u - c\}$  if  $c \leq f_u$ . From Eq. (12) (or (28)), we see that, for  $n \geq 1$ ,  $\lambda_n$  and  $\mu_n$  satisfy

$$\lambda_n + \mu_n = f_u + g_v - c - d\ell_n < 0, \lambda_n \mu_n = D_n := d\ell_n (c - f_u) - cg_v + f_u g_v - g_u f_v.$$
(34)

Note that  $f_u g_v - f_v g_u > 0$ , and for schemes (a) and (b),  $f_u > 0$  and  $g_v < 0$ . Then if  $c \geq f_u$ ,  $D_n > 0$  for any  $n \geq 1$ , which implies that  $\lambda_n$  and  $\mu_n$  both have negative real parts for any  $n \geq 1$ , and (i) and (ii) are proved.

If  $c < f_u$ , then for each  $n \ge 1$ ,  $D_n$  is decreasing with respect to d,  $D_n = 0$  for  $d=d_n$ , and  $D_n<0$  for  $d>d_n$ . Therefore  $\mu_n>0>\lambda_n$  when  $d>d_n$ , and (iii) holds.

Remark 1. We remark that it follows from Theorem 2.3 that for the activatorinhibitor models with a nonlocal activator dispersal and a diffusive inhibitor dispersal, a large nonlocal activator dispersal rate inhibits the formation of patterns. However, when the dispersal rate c is small, the spectrum of the linearized operator  $\mathcal{L}$  with respect to  $(u_*, v_*)$  is similar to the one of ODE-PDE coupled models (which corresponds to the case c=0), see [29, 32, 33]. Specifically, the constant positive steady state  $(u_*, v_*)$  is always linearly unstable, and it could be linearly stable against small disturbances with any wave numbers when the diffusion rate ddecreases.

On the other hand, we have the following results for the stability of  $(u_*, v_*)$  under the schemes (c) and (d), where the dispersal of the inhibitor is nonlocal and the activator has a diffusive dispersal.

**Theorem 2.4.** Assume that  $(u_*, v_*)$  is a constant positive steady state of model (3), the sign pattern of the Jacobian matrix (6) at  $(u_*, v_*)$  is either scheme (c) or (d) defined as in (7), and (5) is satisfied. Then

$$\sigma(\mathcal{L}) = \sigma_p(\mathcal{L}) \cup \sigma_c(\mathcal{L}), \tag{35}$$

where  $\sigma_p(\mathcal{L}) = \{\lambda_n\}_{n=0}^{\infty} \cup \{\mu_n\}_{n=1}^{\infty}, \ \lambda_n, \mu_n \ (n=0,1,2,\cdots) \ are \ defined \ in \ (12), \ and$  $\sigma_c(\mathcal{L}) = \{f_u - c\}.$  Furthermore

(i) If 
$$c \leq \frac{f_u g_v - g_u f_v}{g_v}$$
, then  $\sigma(\mathcal{L}) \subset \mathbb{C}^-$  and  $(u_*, v_*)$  is linearly stable.

(i) If 
$$c \leq \frac{f_u g_v - g_u f_v}{g_v}$$
, then  $\sigma(\mathcal{L}) \subset \mathbb{C}^-$  and  $(u_*, v_*)$  is linearly stable.  
(ii) If  $c > \frac{f_u g_v - g_u f_v}{g_v}$ , then there exists a positive sequence  $\{\tilde{d}_n\}_{n=1}^{\infty}$ , where

$$\tilde{d}_n = \frac{cg_v - f_u g_v + g_u f_v}{(c - f_u)\ell_n} \text{ for } n = 1, 2, 3, \dots,$$
 (36)

such that  $\sigma(\mathcal{L}) \subset \mathbb{C}^-$  and  $(u_*, v_*)$  is linearly stable for  $d > \tilde{d}_1$ , and when  $d \in (\tilde{d}_{n+1}, \tilde{d}_n), \ \mu_j > 0 > \lambda_j \ \text{for any } 1 \leq j \leq n \ \text{and } 0 > \mu_j > \lambda_j \ \text{for any } j \geq n+1.$ 

*Proof.* Since the sign pattern of the Jacobian matrix (6) is either scheme (c) or (d), it follows that  $g_v - f_u > 0$ , which implies that  $c(g_v - f_u + c) - f_v g_u > 0$ . Then, from Theorem 2.2, we see that  $\sigma(\mathcal{L}) = \sigma_p(\mathcal{L}) \cup \sigma_c(\mathcal{L})$ , where  $\sigma_p(\mathcal{L}) = \{\lambda_n\}_{n=0}^{\infty} \cup \{\mu_n\}_{n=1}^{\infty}$ , and  $\sigma_c(\mathcal{L}) = \{f_u - c\}$ . It follows from Eq. (12) (or (28)) that for  $n \geq 1$ ,  $\lambda_n$  and  $\mu_n$ satisfy

$$\lambda_n + \mu_n = f_u + g_v - c - d\ell_n < 0, \lambda_n \mu_n = D_n := d\ell_n (c - f_u) - cg_v + f_u g_v - g_u f_v.$$
(37)

Note that for schemes (c) and (d),  $f_u < 0$  and  $g_v > 0$ . Then if  $c \le \frac{f_u g_v - g_u f_v}{g_v}$ ,  $D_n > 0$  for any  $n \geq 1$ , which implies that  $\lambda_n$  and  $\mu_n$  are both negative for any  $n \ge 1$ , and (i) is proved.

If  $c > \frac{f_u g_v - g_u f_v}{g_v}$ , then for each  $n \ge 1$ ,  $D_n$  is increasing with respect to d,  $D_n = 0$  for  $d = \tilde{d}_n$ , and  $D_n < 0$  for  $d < \tilde{d}_n$ . Hence (ii) holds. 

Remark 2. Theorem 2.4 shows that for the activator-inhibitor models with a nonlocal dispersal of the inhibitor and a diffusive dispersal of the activator, a small nonlocal inhibitor dispersal rate c inhibits the formation of patterns, which is similar to the nonlocal activator and diffusive inhibitor case considered in theme (a) and

(b). However, when the nonlocal inhibitor dispersal rate c is large, the spectrum of the linearized operator  $\mathcal{L}$  with respect to  $(u_*, v_*)$  is similar to that of classical reaction-diffusion model (4). Specifically, the constant positive steady state  $(u_*, v_*)$  is linearly stable for the large diffusion rate d, and it could be linearly unstable against small disturbances of certain wave numbers when the diffusion coefficient d decreases. The number of unstable modes is finite, and it suggests the formation of spatial patterns in these unstable modes.

In the following we will show that  $\{d_j\}_{j=1}^{\infty}$  and  $\{\tilde{d}_j\}_{j=1}^{\infty}$  defined in Theorem 2.3 and 2.4 are all bifurcation points, where nonconstant positive steady states of (3) bifurcate from the constant one. Define the map  $F: X \times \mathbb{R}^+ \to Y$  by

$$F(U,d) = \begin{pmatrix} c\left(\frac{1}{L}\int_0^L u(y)dy - u\right) + f(u,v) \\ dv_{xx} + g(u,v) \end{pmatrix} \text{ for } U = (u,v) \in X, \ d \in \mathbb{R}^+.$$
 (38)

Then  $F(U_*,d)=0$  for any d>0, where  $U_*=(u_*,v_*)$ , and  $\mathcal{L}=\partial_U F(U_*,d)$ , which is the Fréchet derivative of F with respect to U at  $(U_*,d)$ . Furthermore, we define  $\mathcal{L}_j=\partial_U F(U_*,d_j)$  and  $\tilde{\mathcal{L}}_j=\partial_U F(U_*,\tilde{d}_j)$  for  $j\geq 1$ . Then, when the activator has a nonlocal dispersal, we have the following results on the existence of nonconstant positive steady states.

**Theorem 2.5.** Suppose that the assumptions in Theorem 2.3 are satisfied, and  $c < f_u$ . Then, for each positive integer j, the solutions of (8) near  $(d_j, u_*, v_*)$  consist precisely of the curves  $\{(d, u_*, v_*) : d > 0\}$  and  $\{(d_j(s), u_j(s), v_j(s)) : s \in I = (-\delta, \delta)\}$ , where  $d_j(s)$ ,  $u_j(s)$  and  $v_j(s)$  are continuously differentiable functions such that

$$d_j(0) = d_j$$
,  $(u_j(0), v_j(0)) = (u_*, v_*)$ , and  $(u'_j(s), v'_j(s)) = (\phi_{j,+}, \psi_{j,+})$ ,

where

$$(\phi_{j,+}, \psi_{j,+}) = \left\{ \frac{f_v}{c - f_u} \cos \frac{j\pi x}{L}, \cos \frac{j\pi x}{L} \right\}.$$

*Proof.* It follows from Lemma 2.2 that the kernel of  $\mathcal{L}_i$  is

$$\mathcal{N}(\mathcal{L}_i) = \mathcal{N}(\partial_U F(U_*, d_i)) = span\{(\phi_{i,+}, \psi_{i,+})\},\$$

where  $\phi_{j,+}$  and  $\psi_{j,+}$  are defined as in Eq. (14) with  $\mu_j = 0$ . Then we consider the range of  $\mathcal{L}_j$ , denoted by is  $\mathcal{R}(\mathcal{L}_j)$ . From Case 3 in Theorem 2.2, we see that Eq. (16) with  $d = d_j$  and  $\lambda = \mu_j = 0$  has a solution if and only if Eq. (26) with  $d = d_j$  and  $\lambda = \mu_j = 0$  has a solution. Plugging  $d = d_j$  and  $\lambda = \mu_j = 0$  into Eq. (26), we see that (26) has a solution if and only if  $\int_0^L \tilde{\tau} \psi_{j,+} dx = 0$ , which is equivalent to

$$\int_0^L \left[ (f_u - c)\tau_2 - g_u \tau_1 \right] \cos \frac{j\pi x}{L} dx = 0.$$

Therefore,

$$\mathscr{R}(\mathcal{L}_j) = \left\{ (\tau_1, \tau_2) \in Y : \int_0^L \left[ (f_u - c)\tau_2 - g_u \tau_1 \right] \cos \frac{j\pi x}{L} dx = 0 \right\},$$

and consequently  $codim \mathcal{R}(\mathcal{L}_j) = 1$ . A direct calculation yields

$$\partial_{dU} F(U_*, d_j) = \begin{pmatrix} 0 & 0 \\ 0 & \frac{d^2}{dx^2} \end{pmatrix},$$

$$\partial_{dU} F(U_*, d_j) (\phi_{j,+}, \psi_{j,+})^T = (0, \psi''_{j,+}) = (0, -\ell_j \cos \frac{j\pi x}{L}).$$

Then  $-\int_0^L (f_u - c)\ell_j \cos^2 \frac{j\pi x}{L} dx \neq 0$ , which implies that

$$\partial_{dU} F(U_*, d_j)(\phi_{j,+}, \psi_{j,+})^T \notin \mathcal{R}(\mathcal{L}_j).$$

By virtue of the bifurcation from a simple eigenvalue theorem ([10, Theorem 1.7]), we can complete the proof.  $\Box$ 

Here we remark that the bifurcating nonconstant positive steady states obtained in Theorem 2.5 are all linearly unstable from Theorem 2.3 and the eigenvalue perturbation result in [11]. So these nonconstant steady state solutions are not stable patterns which persist for all time.

Similarly, we have the following bifurcation results when the inhibitor has a nonlocal dispersal, and the proof is similar to that of Theorem 2.5 thus it is omitted.

**Theorem 2.6.** Suppose that the assumptions in Theorem 2.4 are satisfied, and  $c > \frac{f_u g_v - g_u f_v}{g_v}$ . Then, for each positive integer j, the solutions of (8) near  $(\tilde{d}_j, u_*, v_*)$  consist precisely of the curves  $\{(d, u_*, v_*) : d > 0\}$  and  $\{(d_j(s), u_j(s), v_j(s)) : s \in I = (-\delta, \delta)\}$ , where  $d_j(s)$ ,  $u_j(s)$  and  $v_j(s)$  are continuously differentiable functions such that

$$d_j(0) = \tilde{d}_j$$
,  $(u_j(0), v_j(0)) = (u_*, v_*)$ , and  $(u'_j(s), v'_j(s)) = (\phi_{j,+}, \psi_{j,+})$ ,

where

$$(\phi_{j,+}, \psi_{j,+}) = \left\{ \frac{f_v}{c - f_u} \cos \frac{j\pi x}{L}, \cos \frac{j\pi x}{L} \right\}.$$

The bifurcating nonconstant positive steady states at  $\tilde{d}_1$  obtained in Theorem 2.6 could be linearly stable from Theorem (2.4) and the eigenvalue perturbation result in [11]. From Theorems 2.4 and 2.6, the spatial pattern formation for (3) under the schemes (c) and (d) is possible for the dispersal parameter pair (c,d) is in the instability region

$$R_2 := \left\{ (c, d) : c > \frac{f_u g_v - g_u f_v}{g_v}, \ d > 0 \right\}.$$
 (39)

And Theorem 2.4 and (36) show that if  $(c,d) \in R_2$ , then  $(u_*, v_*)$  is unstable in the mode–n (corresponding to  $\cos(n\pi x/L)$ ) when the spatial scale satisfies

$$L > n\pi \sqrt{\frac{d(c - f_u)}{cg_v - f_u g_v + g_u f_v}}, \qquad n = 0, 1, 2, 3, \cdots$$
 (40)

To compare the pattern formations in nonlocal dispersal model (3) with the classical reaction-diffusion activator-inhibitor model (4), we revisit the reaction-diffusion activator-inhibitor model (4) and compare the instability regions with respect to parameters c and d for both models (3) and (4), where spatial scale L could induce unstable modes. Here we suppose that all the assumptions for f and g in Theorem 2.4 are satisfied. The characteristic equations with respect to  $(u_*, v_*)$  for model (4) take the following form:

$$\begin{vmatrix} \lambda + c\ell_n - f_u & -f_v \\ -g_u & \lambda + d\ell_n - g_v \end{vmatrix}$$

$$= \lambda^2 - (f_u + g_v - c\ell_n - d\ell_n)\lambda + \tilde{D}(\ell_n) = 0,$$
(41)

for  $n=0,1,2,\cdots$ , where  $\ell_n=\frac{n^2\pi^2}{L^2}$  and

$$\tilde{D}(p) = cdp^2 - (cg_v + df_u)p + f_u g_v - g_u f_v.$$
(42)

Clearly, if  $\Delta(c,d) := (cg_v + df_u)^2 - 4cd(f_ug_v - g_uf_v) > 0$  and  $cg_v + df_u > 0$ , then  $\tilde{D}(p) = 0$  has two positive roots

$$p_{\pm} = \frac{(cg_v + df_u) \pm \sqrt{(cg_v - df_u)^2 + 4cdg_u f_v}}{2cd},$$
(43)

such that D(p) < 0 for  $p \in (p_-, p_+)$ . Therefore, the instability region with respect to parameters c and d for model (4), where the spatial scale could induce instability, takes the following form

$$R_1 := \{(c,d) : c,d > 0, \ \Delta(c,d) > 0, \ cg_v + df_u > 0\} = \{(c,d) : c > d/\alpha_1\},$$
 where

$$\alpha_1 = \frac{f_u g_v - 2g_u f_v - 2\sqrt{(-g_u f_v)(f_u g_v - g_u f_v)}}{f_u^2} > 0.$$

If  $(c,d) \in R_1$ ,  $(u_*, v_*)$  is unstable in the mode-n (corresponding to  $\cos(n\pi x/L)$ ) when the spatial scale L satisfies

$$\frac{n\pi}{\sqrt{p_+}} < L < \frac{n\pi}{\sqrt{p_-}}, \quad n = 1, 2, 3, \cdots$$
(45)

We have the following result on the spectral set of linearized equation of (4) and associated stability problem.

**Theorem 2.7.** Assume that  $(u_*, v_*)$  is a constant positive steady state of model (4), the sign pattern of the Jacobian matrix (6) at  $(u_*, v_*)$  is either scheme (c) or (d) defined as in (7), and (5) is satisfied. Then

$$\sigma(\tilde{\mathcal{L}}) = \sigma_p(\tilde{\mathcal{L}}) = \{\tilde{\lambda}_n\}_{n=0}^{\infty} \cup \{\tilde{\mu}_n\}_{n=0}^{\infty}, \tag{46}$$

where  $\tilde{\mathcal{L}}$  is defined by

$$\tilde{\mathcal{L}}\begin{pmatrix} \phi \\ \psi \end{pmatrix} = \begin{pmatrix} c\phi'' + f_u\phi + f_v\psi \\ d\psi'' + g_u\phi + g_v\psi \end{pmatrix},\tag{47}$$

and  $\tilde{\lambda}_n$  and  $\tilde{\mu}_n$   $(n=0,1,2,3,\cdots)$  are defined by

$$\tilde{\lambda}_{n} = \frac{1}{2} \left( f_{u} + g_{v} - c\ell_{n} - d\ell_{n} - \sqrt{(f_{u} + d\ell_{n} - c\ell_{n} - g_{v})^{2} + 4f_{v}g_{u}} \right),$$

$$\tilde{\mu}_{n} = \frac{1}{2} \left( f_{u} + g_{v} - c\ell_{n} - d\ell_{n} + \sqrt{(f_{u} + d\ell_{n} - c\ell_{n} - g_{v})^{2} + 4f_{v}g_{u}} \right).$$
(48)

Furthermore

- (i) If  $c < d/\alpha_1$ , then  $\sigma(\tilde{\mathcal{L}}) \subset \mathbb{C}^-$  and  $(u_*, v_*)$  is linearly stable.
- (ii) For any c>0, then there exists a sequence  $\{\tilde{d}_n\}_{n=n_0}^{\infty}$ , where

$$n_{0} = \min\{n \in \mathbb{Z} : n > 0, cg_{v}l_{n} - (f_{u}g_{v} - f_{v}g_{u}) > 0\},$$

$$\hat{d}_{n} = \frac{cg_{v}\ell_{n} - f_{u}g_{v} + g_{u}f_{v}}{(c\ell_{n} - f_{u})\ell_{n}} \quad for \quad n = n_{0}, n_{0} + 1, n_{0} + 2, \cdots,$$

$$(49)$$

such that  $\sigma(\tilde{\mathcal{L}}) \subset \mathbb{C}^-$  and  $(u_*, v_*)$  is linearly stable for  $d > \max\{\hat{d}_n\}$ , and when  $d < \max\{\hat{d}_n\}$ ,  $\sigma(\tilde{\mathcal{L}}) \cap \mathbb{C}^+$  has finitely many elements and  $(u_*, v_*)$  is linearly unstable.

Comparing Theorems 2.4 and 2.7, we find that the sets of dispersal parameter pair (c,d) so that the constant steady state  $(u_*,v_*)$  is linearly stable are different: when the inhibitor dispersal is diffusive, the stable parameter set is  $S_1 = \{(c,d): c < d/\alpha_1\}$ ; and when the inhibitor dispersal is nonlocal, the set is  $S_2 = \{(c,d): c < (f_u g_v - g_u f_v)/g_v\}$ . On the other hand, in the complemental set  $R_1$  (defined in

(44)) or  $R_2$  (defined in (39)) (see Fig. 1), spatial pattern formation is possible but the pattern depends on the spatial scale L. For a fixed mode-n, the range of spatial scale for pattern formation in classical reaction-diffusion model (4) is a bounded one (see (45)), while the one for nonlocal dispersal is an unbounded one (see (40)).

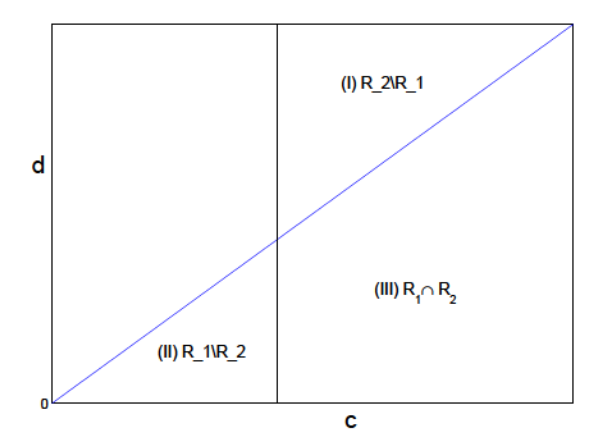


FIGURE 1. Diagram for parameters regions  $R_1$  and  $R_2$ . Here only nonlocal model (3) could exhibit complex patterns in region (I), only reaction-diffusion model (4) could exhibit complex patterns in region (II), and both model (3) and (4) could exhibit complex patterns in region (III).

3. Applications. In this section, we apply the theoretical results in Section 3 to two examples: the Klausmeier-Gray-Scott model of water-plant interaction with nonlocal plant dispersal and the Holling-Tanner predator-prey model with nonlocal predator dispersal.

First, we consider the following Klausmeier-Gray-Scott model of water-plant interaction with nonlocal plant dispersal:

$$\begin{cases} \frac{\partial u}{\partial t} = u^{2}v - bu + c\left(\frac{1}{L}\int_{0}^{L}u(y,t)dy - u(x,t)\right), & 0 \le x \le L, \ t > 0, \\ \frac{\partial v}{\partial t} = A - v - u^{2}v + dv_{xx}, & 0 < x < L, \ t > 0, \\ v_{x}(0,t) = v_{x}(L,t) = 0, & t > 0, \\ u(x,0) = u_{0}(x) \ge 0, \ v(x,0) = v_{0}(x) \ge 0. \end{cases}$$
(50)

This is based on the model of water-plant interaction firstly proposed in [19], with u(x,t) being the density of plant and v(x,t) the density of water. Here A>0 is the precipitation, b>0 is the plant mortality rate, and c,d>0 are the dispersal coefficients. In the original model in [19], the dispersal of plant is diffusive and the one for water is advective. The Gray-Scott model from chemical reaction also has the same functional form [7, 21, 20, 37, 43, 51], so the system (50) is also termed as Klausmeier-Gray-Scott model. A variety of models with the same reaction scheme but other dispersals have been considered: both diffusive [18], and diffusive water

dispersal and nonlocal plant dispersal [1, 12]. The model (50) is a special case of the one in [12] with no advection of water.

The steady states of Eq. (50) satisfy

$$\begin{cases}
-c\left(\frac{1}{L}\int_{0}^{L}u(y)dy - u\right) = u^{2}v - bu, & 0 \le x \le L, \\
-dv'' = A - v - u^{2}v, & 0 < x < L, \\
v'(0) = v'(L) = 0.
\end{cases}$$
(51)

If A > 2b, then model (50) has two constant positive steady states  $(u_1, v_1)$  and  $(u_2, v_2)$ , where

$$u_1 = \frac{A + \sqrt{A^2 - 4b^2}}{2b}, \quad v_1 = \frac{A - \sqrt{A^2 - 4b^2}}{2},$$
$$u_2 = \frac{A - \sqrt{A^2 - 4b^2}}{2b}, \quad v_2 = \frac{A + \sqrt{A^2 - 4b^2}}{2}.$$

The Jacobian matrix with respect to  $(u_i, v_i)$  (i = 1, 2) takes the following form:

$$\begin{pmatrix} f_u & f_v \\ g_u & g_v \end{pmatrix}_{(u_i, v_i)} = \begin{pmatrix} b & u_i^2 \\ -2b & -(u_i^2 + 1) \end{pmatrix},$$

and model (50) is an activator-inhibitor model with a nonlocal dispersal for the activator. It follows from [12] that  $(u_i, v_i)$  is locally asymptotically stable for the corresponding ODEs if  $u_i^2 > \max\{1, b-1\}$ . Since  $u_1 > 1$  and  $u_2 < 1$ , it follows that  $(u_2, v_2)$  is unstable for the corresponding ODEs, and  $(u_1, v_1)$  is locally asymptotically stable for the corresponding ODEs if

$$\left(A + \sqrt{A^2 - 4b^2}\right)^2 > 4b^2(b - 1).$$
(52)

Clearly, if b < 2, Eq. (52) holds. Then, based on Theorems 2.3 and 2.5, we have the following results.

**Proposition 1.** Suppose that A > 2b and Eq. (52) hold, and  $\mathcal{L}$  is the linearized operator with respect to  $(u_1, v_1)$ . Then  $\sigma(\mathcal{L}) = \{\lambda_n\}_{n=0}^{\infty} \cup \{\mu_n\}_{n=1}^{\infty} \cup \{b-c\}$ , where  $\lambda_n, \mu_n(n=0,1,2,3,\cdots)$  are eigenvalues defined in Eq. (12) with  $f_u = b$ ,  $f_v = u_1^2$ ,  $g_u = -2b$  and  $g_v = -(u_1^2 + 1)$ . Furthermore, we have the following three statements.

- (i) If c > b, then  $\sigma(\mathcal{L}) \subset \mathbb{C}^-$  and  $(u_1, v_1)$  is linearly stable.
- (ii) If c = b, then  $\sigma(\mathcal{L}) = \sigma_p(\mathcal{L}) \cup \sigma_c(\mathcal{L})$ , where  $\sigma_p(\mathcal{L}) = \{\lambda_n\}_{n=0}^{\infty} \cup \{\mu_n\}_{n=1}^{\infty} \subset \mathbb{C}^-$ , and  $\sigma_c(\mathcal{L}) = \{0\}$ .
- (iii) If c < b, then  $\sigma(\mathcal{L}) = \sigma_p(\mathcal{L}) \cup \sigma_c(\mathcal{L})$ , where  $\sigma_c(\mathcal{L}) = \{b c\}$ ,  $\sigma_p(\mathcal{L}) = \{\lambda_n\}_{n=0}^{\infty} \cup \{\mu_n\}_{n=1}^{\infty}$ , and  $\sigma_p(\mathcal{L}) \cap \mathbb{C}^+$  has infinitely many elements, so  $(u_1, v_1)$  is unstable with an infinite dimensional unstable space. Furthermore, there exists a sequence  $\{d_j\}_{j=1}^{\infty}$ , where

$$d_j = \frac{(b+c)u_1^2 - b + c}{(b-c)\ell_j} \quad for \quad j = 1, 2, 3, \cdots,$$
 (53)

such that  $\mu_n > 0 > \lambda_n$  for any  $n \ge 1$  when  $d > d_1$ , and when  $d \in (d_{j+1}, d_j)$ ,  $\mu_n > 0 > \lambda_n$  for any  $n \ge j+1$  and  $0 > \mu_n > \lambda_n$  for any  $n \le j$ . For each positive integer j, the solutions of (51) near  $(d_j, u_1, v_1)$  consist precisely of the curves  $\{(d, u_1, v_1) : d > 0\}$  and  $\{(d_j(s), u_j(s), v_j(s)) : s \in I = (-\delta, \delta)\}$ . Here  $d_j(s)$ ,  $u_j(s)$  and  $v_j(s)$  are  $C^{\infty}$  functions such that

$$d_j(0) = d_j, \ (u_j(0), v_j(0)) = (u_1, v_1), \ \text{and} \ (u_j'(s), v_j'(s)) = (\phi_{j,+}, \psi_{j,+}),$$

where

$$(\phi_{j,+}, \psi_{j,+}) = \left(\frac{u_1^2}{c-b}\cos\frac{j\pi x}{L}, \cos\frac{j\pi x}{L}\right).$$

We show some numerical simulations for model (50). We see that a large nonlocal activator dispersal rate inhibits the formation of patterns, see Fig. 2, and complex patterns could occur for small nonlocal activator dispersal rate. Moreover, there exist spike solutions, and the number of spikes could increase as spatial domain L increases, see Figs. 3-4. We remark that similar spike solutions has been investigated in [31] for a nonlocal model without diffusion, which is the case of (50) with c=0. We conjecture that such spike solutions are indeed unstable.

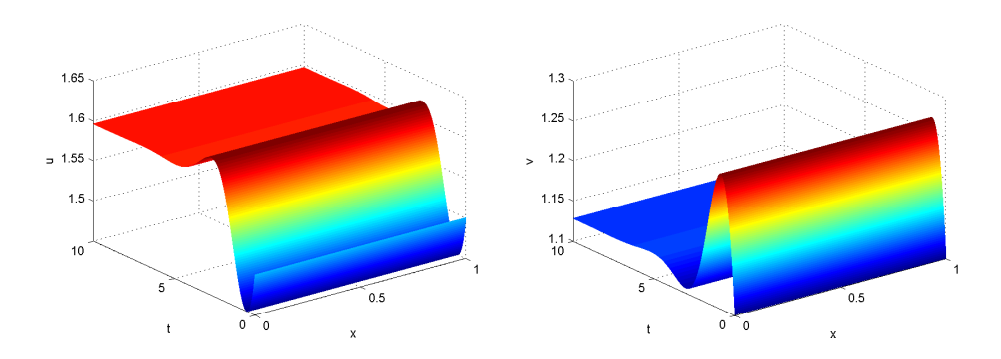


FIGURE 2. The solution of model (50) converges to the constant positive equilibrium  $(u_1, v_1)$  for c > b. Here d = 6, A = 4, b = 1.8, L = 1, c = 10, and the initial values u(x, 0) = 1.5 + 0.001x(1 - x), and  $v(x, 0) = 1.1 + 0.001\cos x$ . (Left) u(x, t); (Right) v(x, t).

Next we consider the activator-inhibitor model with a nonlocal dispersal for the inhibitor, and choose the following nonlocal Holling-Tanner predator-prey model as an example:

$$\begin{cases} \frac{\partial u}{\partial t} = c \left( \frac{1}{L} \int_{0}^{L} u(y, t) dy - u \right) + su \left( 1 - \frac{u}{v} \right), & 0 \le x \le L, \ t > 0, \\ \frac{\partial v}{\partial t} = dv_{xx} + v \left( 1 - \beta v \right) - \frac{muv}{v+1}, & 0 < x < L, \ t > 0, \\ v_{x}(0, t) = v_{x}(L, t) = 0, & t > 0, \\ u(x, 0) = u_{0}(x) > 0, \ v(x, 0) = v_{0}(x) > 0, \end{cases}$$
(54)

where u(x,t) and v(x,t) represent the densities of the predator and prey at location x and time t respectively, and parameters  $\beta$ , m, c, d and s are all positive, see [49] for more detailed biological meanings. The steady states of model (54) satisfy

$$\begin{cases}
-c\left(\frac{1}{L}\int_{0}^{L}u(y)dy - u\right) = su\left(1 - \frac{u}{v}\right), & 0 \le x \le L, \\
-dv'' = v\left(1 - \beta v\right) - \frac{muv}{v+1}, & 0 < x < L, \\
v'(0) = v'(L) = 0.
\end{cases}$$
(55)

Clearly, model (54) has a unique constant positive steady state for any c, d > 0, denoted by  $(u_*, v_*)$ , where  $v_*$  satisfies  $(1 - \beta v_*)(1 + v_*) = mv_*$ , and  $u_* = v_*$ .

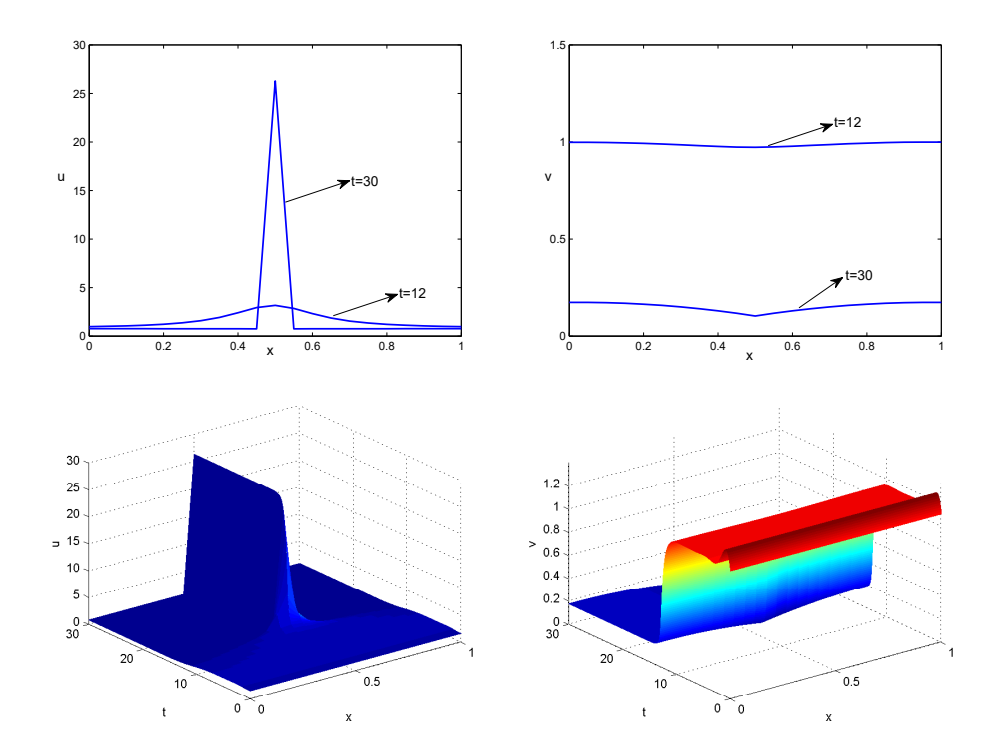


FIGURE 3. The solution of model (50) forms a one-spike spatial pattern for c < b, and the upper panels show the profile of u and v at time t = 12 and t = 30, respectively. Here d = 6, A = 4, b = 1.8, L = 1, c = 1, and the initial values u(x, 0) = 1.5 + 0.001x(1 - x), and  $v(x, 0) = 1.1 + 0.001\cos x$ . (Left) u(x, t); (Right) v(x, t).

It follows from [28] that the Jocobian matrix with respect to  $(u_*, v_*)$  takes the following form:

$$\left(\begin{array}{cc} f_u & f_v \\ g_u & g_v \end{array}\right)_{(u_*,v_*)} = \left(\begin{array}{cc} -s & s \\ -\frac{mv_*}{1+v_*} & s_0 \end{array}\right),$$

the determinate  $(f_u g_v - f_v g_u)|_{(u_*,v_*)} = \frac{s(1+\beta v_*^2)}{1+v_*} > 0$ ,  $s_0 = -\beta v_* + \frac{mv_*^2}{(v_*+1)^2}$ , and  $s_0 > 0$  if and only if

$$\beta < 1 \text{ and } m > \frac{(1+\beta)^2}{2(1-\beta)}.$$
 (56)

Similarly, based on Theorems 2.4 and 2.6, we have the following results.

**Proposition 2.** Suppose that  $\beta$  and m satisfy Eq. (56),  $s > s_0$ , and  $\mathcal{L}$  is the linearized operator with respect to  $(u_*, v_*)$ . Then

$$\sigma(\mathcal{L}) = \sigma_p(\mathcal{L}) \cup \sigma_c(\mathcal{L}), \tag{57}$$

where  $\sigma_p(\mathcal{L}) = \{\lambda_n\}_{n=0}^{\infty} \cup \{\mu_n\}_{n=1}^{\infty}, \ \lambda_n, \mu_n(n=0,1,2,\cdots) \ are \ defined in (12) with <math>f_u = -s, \ f_v = s, \ g_u = -\frac{mv_*}{1+v_*} \ and \ g_v = s_0, \ and \ \sigma_c(\mathcal{L}) = \{f_u - c\}.$  Furthermore,

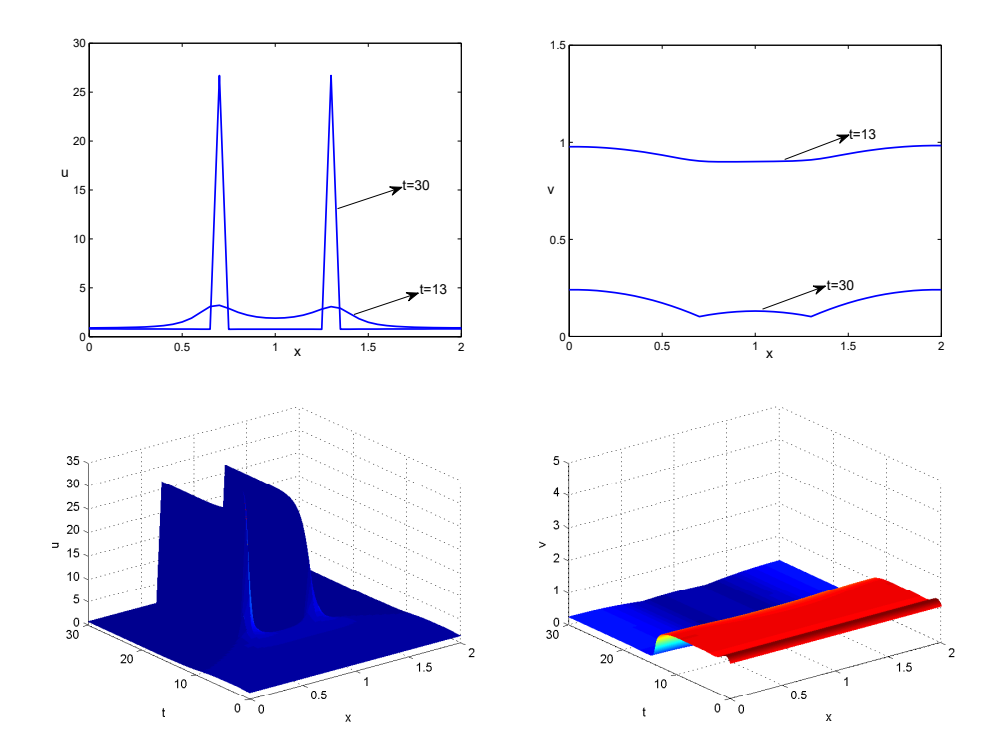


FIGURE 4. The solution of model (50) forms to a two-spike spatial pattern for c < b, and the upper panels show the profile of u and v at time t = 13 and t = 30, respectively. Here d = 6, A = 4, b = 1.8, L = 2, c = 1, and the initial values u(x,0) = 1.5 + 0.001x(2-x), and  $v(x,0) = 1.1 + 0.001\cos x$ . (Left) u(x,t); (Right) v(x,t).

- (i) If  $c \leq c_0 := \frac{s(1+\beta v_*^2)}{s_0(1+v_*)}$ , then  $\sigma(\mathcal{L}) \subset \mathbb{C}^-$ .
- (ii) If  $c > c_0$ , then there exists a sequence  $\{\tilde{d}_j\}_{j=1}^{\infty}$ , where

$$\tilde{d}_{j} = \frac{1}{(c+s)\ell_{j}} \left[ cs_{0} - \frac{s(1+\beta v_{*}^{2})}{(1+v_{*})} \right] \quad for \quad j = 1, 2, 3, \cdots,$$
 (58)

such that  $\sigma(\mathcal{L}) \subset \mathbb{C}^-$  for  $d > \tilde{d}_1$ , and  $\mu_n > 0 > \lambda_n$  for any  $n \leq j$  and  $0 > \mu_n > \lambda_n$  for any  $n \geq j+1$  when  $d \in (\tilde{d}_{j+1}, \tilde{d}_j)$ . Moreover, for each positive integer j, the solutions of (55) near  $(\tilde{d}_j, u_*, v_*)$  consist precisely of the curves  $\{(d, u_*, v_*) : d > 0\}$  and  $\{(d(s), u_j(s), v_j(s)) : s \in I = (-\delta, \delta)\}$ , where d(s),  $u_j(s)$  and  $v_j(s)$  are  $C^{\infty}$  functions such that

$$d(0) = \tilde{d}_j$$
,  $(u_j(0), v_j(0)) = (u_*, v_*)$ , and  $(u'_j(s), v'_j(s)) = (\phi_{j,+}, \psi_{j,+})$ , where

$$(\phi_{j,+}, \psi_{j,+}) = \left(\frac{s}{c+s}\cos\frac{j\pi x}{L}, \cos\frac{j\pi x}{L}\right).$$

Now, we give some numerical simulations for model (54), and it is different from model (50). For this case, a small nonlocal dispersal rate c inhibits the formation of patterns, and complex patterns could occur for a large nonlocal dispersal rate

c, see Fig. 5. Furthermore, we also show that if  $(c,d) \in R_2 \backslash R_1$ , where  $R_1$  and  $R_2$  are defined as in Eqs. (44) and (39) respectively, then a large spatial scale will induce complex patterns for the nonlocal model (54), whereas  $(u_*, v_*)$  is locally asymptotically stable for the corresponding reaction-diffusion model

$$\begin{cases}
\frac{\partial u}{\partial t} = cu_{xx} + su\left(1 - \frac{u}{v}\right), & 0 \le x \le L, \ t > 0, \\
\frac{\partial v}{\partial t} = dv_{xx} + v\left(1 - \beta v\right) - \frac{muv}{v+1}, & 0 < x < L, \ t > 0, \\
u_{x}(0, t) = u_{x}(L, t) = v_{x}(0, t) = v_{x}(L, t) = 0, \quad t > 0, \\
u(x, 0) = u_{0}(x) > 0, \quad v(x, 0) = v_{0}(x) > 0,
\end{cases}$$
(59)

see Fig. 6.

4. **Discussion.** In this paper, we consider the spatial pattern formation for activator inhibitor models with nonlocal dispersal. The nonlocal dispersal is chosen to be the "spatial averaging" dispersal, which is an approximation of a general nonlocal dispersal with large dispersal scale.

It is shown that if the dispersal of the activator is nonlocal and the one for the inhibitor is diffusive, then a large nonlocal activator dispersal rate c inhibits the formation of spatial patterns, and a small activator dispersal rate c induces the instability, and complex spatial patterns could occur. Similar to the pattern formation scenario of coupled ODE-PDE systems, these non-constant steady states generated from symmetry-breaking bifurcations are unstable. But for the Klausmeier water-plant model, spike layer solutions are still numerically observed, and the number of spikes increases as the size L of the spatial domain increases, see Fig. 3 and 4. The persistence mechanism of such spike layer solutions requires further investigation.

On the other hand, if the dispersal of the activator is diffusive and the one for the inhibitor is nonlocal, then a small nonlocal inhibitor dispersal rate c inhibits the formation of spatial patterns; while a large nonlocal inhibitor dispersal rate c induces instability, and complex spatial patterns could occur. This pattern formation scenario is similar to the Turing instability for the classical reaction-diffusion model (4), and the non-constant steady states generated from symmetry-breaking bifurcations could be stable ones. However, the nonlocal dispersal induced pattern formation occurs in a different instability parameter regime compared to the Turing mechanism, so that is a new mechanism for spatial pattern formation. We should point out that the theoretical results obtained in this paper could also apply to models in a higher dimensional domain as along as the eigenvalues of the Laplacian operator are simple.

The pattern formation mechanism revealed in this paper applies to the case when the dispersal scale of either the activator or the inhibitor is large (or nonlocal), while in the original Turing reaction-diffusion model, the dispersal scales of both the activator and the inhibitor are small (or local). Our results show the effect of these two different dispersal scenarios on the formation of spatial patterns. It should be noted that here the dispersal is assumed to be symmetric and there is no population loss in the dispersal. In reality the wind directions may produce non-symmetric distribution, and the population loss occurring in the dispersal could also affect the spatial patterns. Moreover, the analysis in this paper cannot work for other kernel functions, since the methods here works as the constant kernel induces a rank-1 linear mapping. The nonlocal dispersal will make the associated solution

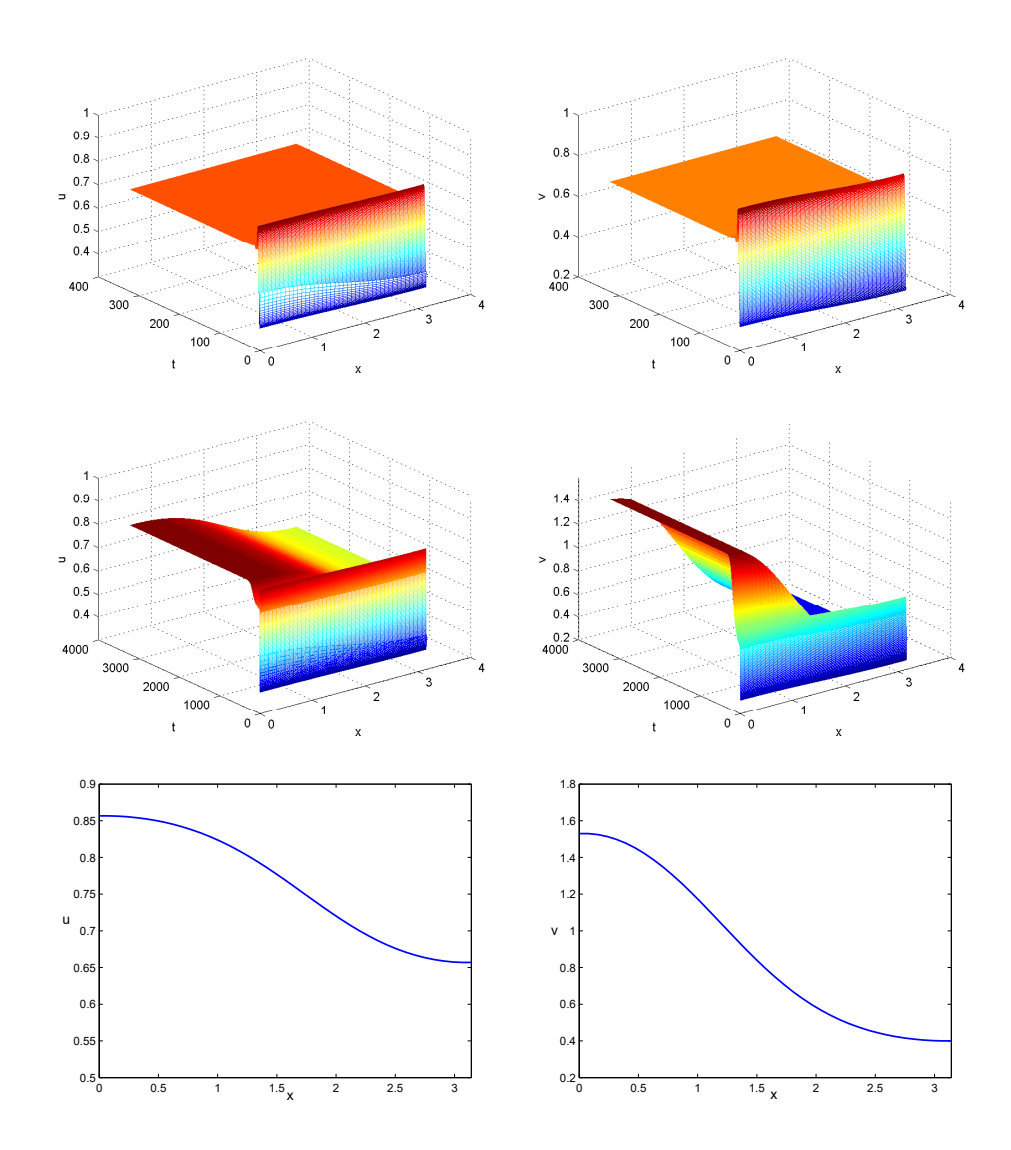


FIGURE 5. The solution of model (54) converges to the constant steady state (respectively, a nonconstant stationary pattern) for  $c < c_0$  (respectively,  $c > c_0$ ), and the lower panel show the profile of the nonconstant stationary pattern with c=4. Here  $\beta=0.2$ , m=2,  $L=\pi$ , s=1, d=0.03, and the initial values  $u(x,0)=0.5+0.05\cos x$ , and  $v(x,0)=0.3+0.02\cos x$ . (Upper) c=2; (Middle) c=4; (Left) u(x,t); (Right) v(x,t).

semiflow noncompact, and consequently it will bring some difficulties to analyze the global dynamics of model (3). These questions will be considered in the future investigations.

**Acknowledgments.** We would like to thank the anonymous reviewer for helpful comments which improve the manuscript.

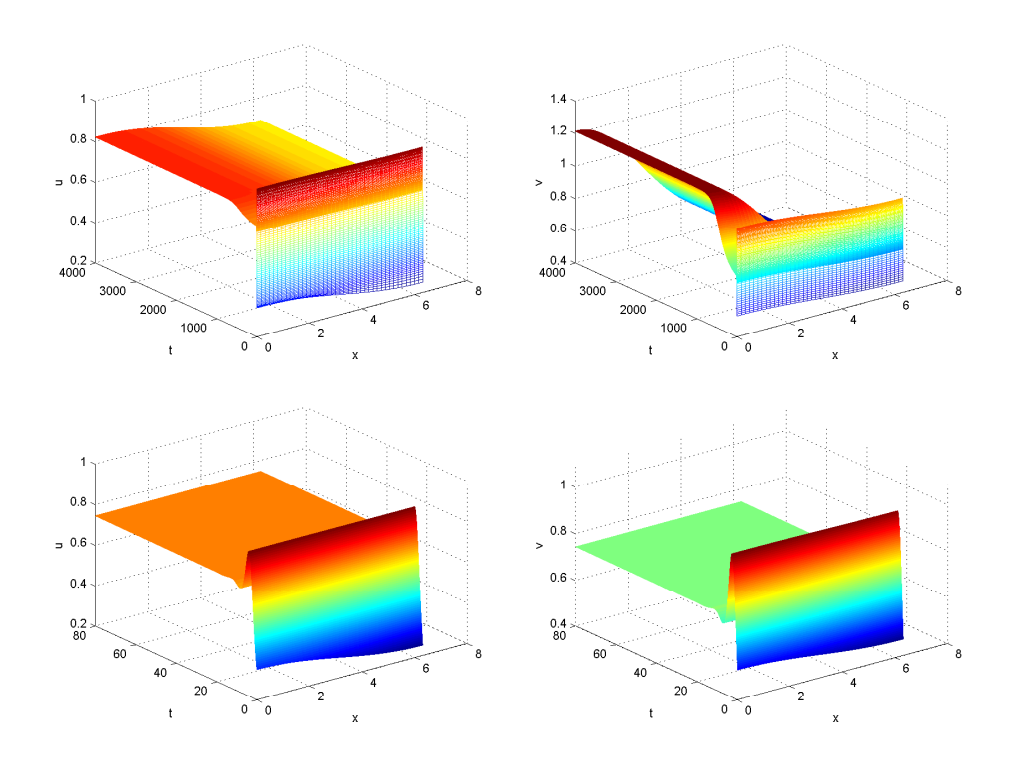


FIGURE 6. The solution converges to a nonconstant stationary pattern for the nonlocal model (54), whereas the solution converges to the constant steady state for the reaction-diffusion model (59). Here the initial values  $u(x,0) = 0.3 + 0.05 \cos x/2$ , and  $v(x,0) = 0.5 + 0.03 \cos x/2$ ,  $\beta = 0.2$ , m = 2,  $L = 2\pi$ , s = 1, d = 0.15, c = 4, and  $(c,d) \in R_2 \backslash R_1$ , where  $R_1$  and  $R_2$  are defined as in Eqs. (44) and (39), respectively. (Left) u(x,t); (Right) v(x,t).

#### REFERENCES

- M. Alfaro, H. Izuhara and M. Mimura, On a nonlocal system for vegetation in drylands, J. Math. Biol., 77 (2018), 1761–1793.
- [2] E. J. Allen, L. J. S. Allen and X. Gilliam, Dispersal and competition models for plants, J. Math. Biol., 34 (1996), 455–481.
- [3] L. J. S. Allen, E. J. Allen and S. Ponweera, A mathematical model for weed dispersal and control, Bull. Math. Biol., 58 (1996), 815–834.
- [4] X. L. Bai and F. Li, Global dynamics of a competition model with nonlocal dispersal II: The full system, J. Differential Equations, 258 (2015), 2655–2685.
- [5] X.-L. Bai and F. Li, Classification of global dynamics of competition models with nonlocal dispersals I: symmetric kernels, Calc. Var. Partial Differential Equations, 57 (2018), 35pp.
- [6] K. J. Brown and F. A. Davidson, Global bifurcation in the Brusselator system, Nonlinear Anal., 24 (1995), 1713–1725.
- [7] W. Chen and M. J. Ward, The stability and dynamics of localized spot patterns in the twodimensional Gray-Scott model, SIAM J. Appl. Dyn. Syst., 10 (2011), 582–666.
- [8] J. Coville, On a simple criterion for the existence of a principal eigenfunction of some nonlocal operators, J. Differential Equations, 249 (2010), 2921–2953.
- [9] J. Coville, J. Dávila and S. Martínez, Existence and uniqueness of solutions to a nonlocal equation with monostable nonlinearity, SIAM J. Math. Anal., 39 (2008), 1693–1709.

- [10] M. G. Crandall and P. H. Rabinowitz, Bifurcation from simple eigenvalues, J. Functional Analysis, 8 (1971), 321–340.
- [11] M. G. Crandall and P. H. Rabinowitz, Bifurcation, perturbation of simple eigenvalues and linearized stability, Arch. Rational Mech. Anal., 52 (1973), 161–180.
- [12] L. Eigentler and J. A. Sherratt, Analysis of a model for banded vegetation patterns in semiarid environments with nonlocal dispersal, J. Math. Biol., 77 (2018), 739–763.
- [13] J. García-Melián and J. D. Rossi, On the principal eigenvalue of some nonlocal diffusion problems, J. Differential Equations, 246 (2009), 21–38.
- [14] A. Gierer and H. Meinhardt, A theory of biological pattern formation, Kybernetik, 12 (1972), 30–39.
- [15] V. Hutson, S. Martinez, K. Mischaikow and G. T. Vickers, The evolution of dispersal, J. Math. Biol., 47 (2003), 483–517.
- [16] J. Jang, W.-M. Ni and M.-X. Tang, Global bifurcation and structure of Turing patterns in the 1-D Lengyel-Epstein model, J. Dynam. Differential Equations, 16 (2004), 297–320.
- [17] J.-Y. Jin, J.-P. Shi, J.-J. Wei and F.-Q. Yi, Bifurcations of patterned solutions in the diffusive Lengyel-Epstein system of CIMA chemical reactions, Rocky Mountain J. Math., 43 (2013), 1637–1674.
- [18] B. J. Kealy and D. J. Wollkind, A nonlinear stability analysis of vegetative Turing pattern formation for an interaction-diffusion plant-surface water model system in an arid flat environment, Bull. Math. Biol., 74 (2012), 803–833.
- [19] C. A. Klausmeier, Regular and irregular patterns in semiarid vegetation, Science, 284 (1999), 1826–1828.
- [20] T. Kolokolnikov, M. J. Ward and J.-C. Wei, The existence and stability of spike equilibria in the one-dimensional Gray-Scott model: The low feed-rate regime, Stud. Appl. Math., 115 (2005), 21–71.
- [21] T. Kolokolnikov, M. J. Ward and J.-C. Wei, The existence and stability of spike equilibria in the one-dimensional Gray-Scott model: The pulse-splitting regime, *Phys. D*, 202 (2005), 258–293.
- [22] S. Kondo and R. Asai, A reaction-diffusion wave on the skin of the marine angelfish Pomacanthus, Nature, 376 (1995), 765-768.
- [23] S. Kondo and T. Miura, Reaction-diffusion model as a framework for understanding biological pattern formation, Science, 329 (2010), 1616–1620.
- [24] M. Kot, M. A. Lewis and P. van den Driessche, Dispersal data and the spread of invading organisms, Ecology, 77 (1996), 2017–2042.
- [25] I. Lengyel and I. R. Epstein, Modeling of Turing structures in the chlorite-iodide-malonic acid-starch reaction system, Science, 251 (1991), 650–652.
- [26] F. Li, Y. Lou and Y. Wang, Global dynamics of a competition model with non-local dispersal I: The shadow system, J. Math. Anal. Appl., 412 (2014), 485–497.
- [27] S.-B. Li, J.-H. Wu and Y.-Y. Dong, Turing patterns in a reaction-diffusion model with the Degn-Harrison reaction scheme, J. Differential Equations, 259 (2015), 1990–2029.
- [28] X. Li, W.-H. Jiang and J.-P. Shi, Hopf bifurcation and Turing instability in the reactiondiffusion Holling-Tanner predator-prey model, IMA J. Appl. Math., 78 (2013), 287–306.
- [29] Y. Li, A. Marciniak-Czochra, I. Takagi and B.-Y. Wu, Bifurcation analysis of a diffusion-ODE model with Turing instability and hysteresis, *Hiroshima Math. J.*, 47 (2017), 217–247.
- [30] F. Lutscher, E. Pachepsky and M. A. Lewis, The effect of dispersal patterns on stream populations, SIAM Rev., 47 (2005), 749–772.
- [31] A. Marciniak-Czochra, S. Härting, G. Karch and K. Suzuki, Dynamical spike solutions in a nonlocal model of pattern formation, *Nonlinearity*, **31** (2018), 1757–1781.
- [32] A. Marciniak-Czochra, G. Karch and K. Suzuki, Unstable patterns in reaction-diffusion model of early carcinogenesis, J. Math. Pures. Appl. (9), 99 (2013), 509–543.
- [33] A. Marciniak-Czochra, G. Karch and K. Suzuki, Instability of Turing patterns in reaction-diffusion-ODE systems, J. Math. Biol., 74 (2017), 583-618.
- [34] J. Medlock and M. Kot, Spreading disease: Integro-differential equations old and new, Math. Biosci., 184 (2003), 201–222.
- [35] W.-M. Ni and M.-X. Tang, Turing patterns in the Lengyel-Epstein system for the CIMA reaction, Trans. Amer. Math. Soc., 357 (2005), 3953–3969.
- [36] A. Pazy, Semigroups of Linear Operators and Applications to Partial Differential Equations, Applied Mathematical Sciences, 44, Springer-Verlag, New York, 1983.
- [37] J. E. Pearson, Complex patterns in a simple system, Science, 261 (1993), 189-192.

- [38] R. Peng, F.-Q. Yi and X.-Q. Zhao, Spatiotemporal patterns in a reaction-diffusion model with the Degn-Harrison reaction scheme, *J. Differential Equations*, **254** (2013), 2465–2498.
- [39] J. A. Powell and N. E. Zimmermann, Multiscale analysis of active seed dispersal contributes to resolving Reid's paradox, Ecology, 85 (2004), 490–506.
- [40] M. Rietkerk, M. C. Boerlijst, F. van Langevelde and R. HilleRisLambers, et al., Self-organization of vegetation in arid ecosystems, Amer. Naturalist, 160 (2002), 524–530.
- [41] M. Rietkerk, S. C. Dekker, P. C. De Ruiter and J. van de Koppel, Self-organized patchiness and catastrophic shifts in ecosystems. *Science*, 305 (2004), 1926–1929.
- [42] L. A. Segel and J. L. Jackson, Dissipative structure: An explanation and an ecological example, J. Theor. Biol., 37 (1972), 545–559.
- [43] L. Sewalt and A. Doelman, Spatially periodic multipulse patterns in a generalized Klausmeier-Gray-Scott model, SIAM J. Appl. Dyn. Syst., 16 (2017), 1113–1163.
- [44] W.-X. Shen and X.-X. Xie, On principal spectrum points/principal eigenvalues of nonlocal dispersal operators and applications, Discrete Contin. Dyn. Syst., 35 (2015), 1665–1696.
- [45] R. Sheth, L. Marcon, M. F. Bastida and M. Junco, et al., Hox genes regulate digit patterning by controlling the wavelength of a Turing-type mechanism, *Science*, **338** (2012), 1476–1480.
- [46] S. Sick, S. Reinker, J. Timmer and T. Schlake, WNT and DKK determine hair follicle spacing through a reaction-diffusion mechanism, *Science*, 314 (2006), 1447–1450.
- [47] J.-W. Sun, W.-T. Li and Z.-C. Wang, The periodic principal eigenvalues with applications to the nonlocal dispersal logistic equation, *J. Differential Equations*, **263** (2017), 934–971.
- [48] J.-W. Sun, W.-T. Li and F.-Y. Yang, Blow-up profiles for positive solutions of nonlocal dispersal equation, Appl. Math. Lett., 42 (2015), 59–63.
- [49] J. T. Tanner, The stability and the intrinsic growth rates of prey and predator populations, Ecology, 56 (1975), 855–867.
- [50] A. M. Turing, The chemical basis of morphogenesis, Philos. Trans. Roy. Soc. London Ser. B, 237 (1952), 37–72.
- [51] S. van der Stelt, A. Doelman, G. Hek and J. D. M. Rademacher, Rise and fall of periodic patterns for a generalized Klausmeier-Gray-Scott model, J. Nonlinear Sci., 23 (2013), 39–95.
- [52] J.-F. Wang, Spatiotemporal patterns of a homogeneous diffusive predator-prey system with Holling type III functional response, *J. Dynam. Differential Equations*, **29** (2017), 1383–1409.
- [53] J.-F. Wang, J.-P. Shi and J.-J. Wei, Dynamics and pattern formation in a diffusive predatorprey system with strong Allee effect in prey, J. Differential Equations, 251 (2011), 1276–1304.
- [54] F.-Q. Yi, J.-J. Wei and J.-P. Shi, Bifurcation and spatiotemporal patterns in a homogeneous diffusive predator-prey system, *J. Differential Equations*, **246** (2009), 1944–1977.

Received July 2019; revised October 2019.

E-mail address: chenss@hit.edu.cn E-mail address: jxshix@wm.edu E-mail address: zgh711@swu.edu.cn